Tetrahedron 68 (2012) 6231–6239

Contents lists available at SciVerse ScienceDirect

Tetrahedron

journal homepage: www.elsevier.com/locate/tet

Hydrogen-bond-assisted supramolecular 1-D tape-like structures of mesogenic bis-pyrazoles

Huei-Yun Lin [c], Hsiu-Ming Kuo [c], Shao-Gang Wen [c], Hwo-Shuenn Sheu [a], Gene-Hsiang Lee [b], Chung K. Lai [c,*]

[a] National Synchrotron Radiation Research Center, Hsinchu 30077, Taiwan, ROC
[b] Instrumentation Center, National Taiwan University, Taipei 10660, Taiwan, ROC
[c] Department of Chemistry, National Central University, Chung-Li 32001, Taiwan, ROC

ARTICLE INFO

Article history:
Received 8 April 2012
Received in revised form 9 May 2012
Accepted 15 May 2012
Available online 24 May 2012

ABSTRACT

Two new series of isomeric bis-pyrazoles **1a**–**b** are prepared, characterized, and their mesomorphic properties investigated. These pyrazoyl derivatives were obtained from the condensation of α,β-diketones **2a**–**b** with hydrazine monohydrate in refluxing THF. Two single crystallographic structures of compounds mesogenic **1a** (n=14) and nonmesogenic **1b** (n=8) were determined by X-ray analysis. Both **1a**–**14** and **1b**–**8** crystallize in a triclinic space group $P\bar{1}$ and monoclinic $C2/c$ group, respectively. An extended H-bonded structure was formed in both crystal lattices, giving a pseudo 1D-polymeric tape-like structure. Derivatives **1a** exhibited smectic A/C mesophases, in contrast, derivatives **1b** were all non-mesogenic. The difference in mesomorphic behavior was attributed to the between linear conformation and the coplanarity of the five rings over than in **1a**. The correlation between the molecular structures and the mesomorphic properties is discussed.

1. Introduction

Using H-bonds have now become an important concept to construct novel molecular architectures[1–5] with liquid crystalline and/or other optic-electric properties. Many unique mesogenic structures[6–10] induced or stabilized by H-bonded were already known, in which either intermolecular or/and intramolecular H-bonds were widely applied. However, H-bonds, compared to covalent bonds are relatively weak; they are sensitive to the structural alternation, and any puny deviation in molecular structures might have a dramatic impact on the propensity of these H-bond stabilized molecules.[11,12] Using H-bonded interaction can be twofold; complementary shapes and intermolecular force. A better or/and preferable molecular shape formed by a dimeric, trimeric or polymeric structure can be created, leading to an appropriate aspect ratio required to form potential mesogens. This concept was often used and observed for organic molecules with unconventionally shapes. Secondly, intermolecular interactions enhanced by induced H-bonds usually facilitate the formation of mesophases, particularly for those molecules with no dipole group substituted. Nevertheless, the interplay between intermolecular attraction and packing is generally obscured by the molecular structures in designing liquid crystal.

Pyrazoles, usually considered as an important member among aromatic N-heterocycles have attracted substantial studies during the past decades, particularly in the field of biological chemistries.[13–15] Part of which stems from their capability of forming conjugate bases, pyrazoylates and N-substituted derivatives. Pyrazoles are also considered electronically as both σ-donor and π-acceptor ligands.[16] In addition, their capabilities of binding transition metals in a variety of coordination modes[17–19] are truly robust. Moreover, the pyrazoyl-hydrogen (−NH) can capably act as a hydrogen-bond donor, which makes the pyrazoles as an excellent candidate in supramolecular chemistry.[20] Such intermolecular hydrogen bondings are relatively strong, and many examples with a dimeric structure was often obtained in many pyrazoylate systems.[21] Also, a trimeric, tetrameric,[22] hexameric and catmeric structures aggregated in the solid states were found.

However, known examples prepared for material chemistry has been relatively lesser though they are thermally and hydrolytically very stable. Only few examples of mesogenic pyrazoles[23–26] and their derived metallomesogens[27–30] were prepared since first example reported in 1992. Some of such metallomesogens[31a] exhibited a unique red-luminescent behavior or organogel.[31b] A few examples of symmetrical and unsymmetrical mono-pyrazoles and their metallomesogens were developed and studied by this group.

* Corresponding author. Tel.: +886 3 4259207; fax: +886 3 4277972; e-mail address: cklai@cc.ncu.edu.tw (C.K. Lai).

0040-4020/$ – see front matter © 2012 Elsevier Ltd. All rights reserved.
doi:10.1016/j.tet.2012.05.060

The exocyclic bond angles resulted from the incorporation of heterocyclic rings as core group played an important role in induction/formation of mesomorphic behavior. In this work, two homolog series of bis-pyrazoles **1a**–**b** were prepared, characterized and mesomorphic properties studied. Both compounds **1a**–**b** are in fact structural isomers. Compounds **1a** were all mesogenic, giving SmA/SmC phases, whereas all compounds **1b** were not mesogenic. Two single crystals **1a**–**14** and **1b**–**8** were also resolved and analyzed. The correlation between crystal data and molecular structures was performed to aim in understanding the relationship between the structures and the mesomorphic properties. The example illustrated a supramolecular assembly by bis-pyrazole-based materials, in which an extended 1D non-covalent bonding network in the solid/LC states was observed.

2. Results and discussion

2.1. Synthesis and characterization

The synthetic routes[21b,32–37] used to prepare bis(pyrazoles) **1a**–**b** are listed in Scheme 1. The bis-diketones **2a**–**b** were synthesized by double condensation of dimethyl terephthalate or dimethyl isophthalate, the appropriate acetophenone derivatives and sodium hydride NaH in refluxing THF or dimethoxethane for 24 h under nitrogen atmosphere. The yields were modest, ranged from 45–65%. They exist possibly in a few different keto–enol tautomeric forms. All compounds were characterized by ^{1}H and ^{13}C NMR spectroscopy. On the ^{1}H NMR spectra, two singlet peaks appeared at δ 6.81–6.84 and δ 16.87–17.08 is characteristically assigned for olefinic-H (−COH=C*H*) and enol-H (=CH−O*H*) groups of compounds **2a**–**b**. The bis-pyrazoles **1a**–**b** were obtained by the reactions of bis-diketones **2a**–**b** with excess hydrazine monohydrate in refluxing THF. These compounds **1a**–**b** isolated as white solid were obtained by recrystallization from warm THF. The solubility of all pyrazoles **1a**–**b** were relatively poor in THF at room temperature, therefore, most of final pyrazoles were only characterized by ^{1}H NMR spectroscopy. The formation of final pyrazoles was monitored by the disappearance of a singlet at δ 16.87–17.08 assigned for −CHCOH. In addition, a characteristic peak at δ 10.25–10.91 and 12.37–13.37 assigned to the pyrazole-*H* (−NH) was observed. The exchange experiment of pyrazoles with D_2O solvent was also performed to confirm the assignment of two pyrazole-H peaks. The intensities of these two peaks were all apparently decreased while the peaks were only slightly shifted to δ 12.47 and 10.99, for example, **1b** (n=8) after addition of a drop D_2O for 7 h. The elemental analyses of compounds **1a**–**b** were all performed to confirm their purities.

2.2. Phase transitions, mesomorphic behavior and thermal stabilities

The thermal behavior of compounds **1a**–**b** and **2a**–**b** was investigated by polarized optical microscopy and differential scanning calorimetry. The transition temperatures and enthalpies of the compounds **1**–**2** are listed in Table 1. All bis-diketones **2a**–**b** were nonmesogenic. A phase transition of crystal-to-isotropic was observed, for example, at T_{mp}=156.9 °C and 119.1 °C, respectively, for compound **2a** (n=12) and **2b** (n=12). Compounds **2a** have higher clearing temperatures than those of **2b** (n=12) due to molecular linearity symmetry. The lack of mesomorphism in **2a**–**b** might be attributed to the pronounced non-bending linearity observed in similar symmetric β-diketonate systems. An improved mesophase was often obtained by an introduction of a polar group incorporated, such as −CN group. Polar groups can better prefer an antiparallel arrangement. In contrast, all derivatives **1a** (n=8, 10, 12, 14, 16) exhibited an enantiotropic mesomorphic behavior, whereas all other derivatives **1b** (n=8, 10, 12, 14) showed crystal phases. Under optical microscope, compounds **1a** exhibited fan-shaped textures at higher temperatures and Schlieren textures at lower temperatures (Fig. 1). These two textures were characteristic of a layer smectic A and C phase expected for the rod-like molecules. Under optical microscope, a large area of homeotropic domains was also observed for SmA phase. The clearing temperatures were all ranged at T_{cl}=374.6 (n=8)–309.4 °C (n=16) while the melting temperatures remained at T_{mp}=201.2 (n=8)–185.7 °C (n=16). On the other hand, the temperature range of mesophases decreased with longer carbon length of alkoxy chains, ΔT_m=187.2 (n=8)> 155.0 (n=12)>127.1 °C (n=16) on cooling process. The transition enthalpies of SmA-to-iso phases also decreased with carbon length. In contrast, all derivatives **1b** were not mesogenic. A transition of crystal-to-isotropic for **1b** was observed. Surprisingly, all melting temperatures of **1b** were much lower than those of homologs of **1a** by ca. T=170.5 (n=8)–128.1 °C (n=14). Compounds **1a** and **1b** are structurally isomeric. The larger difference on the clearing temperatures might probably be due to the better linearity and

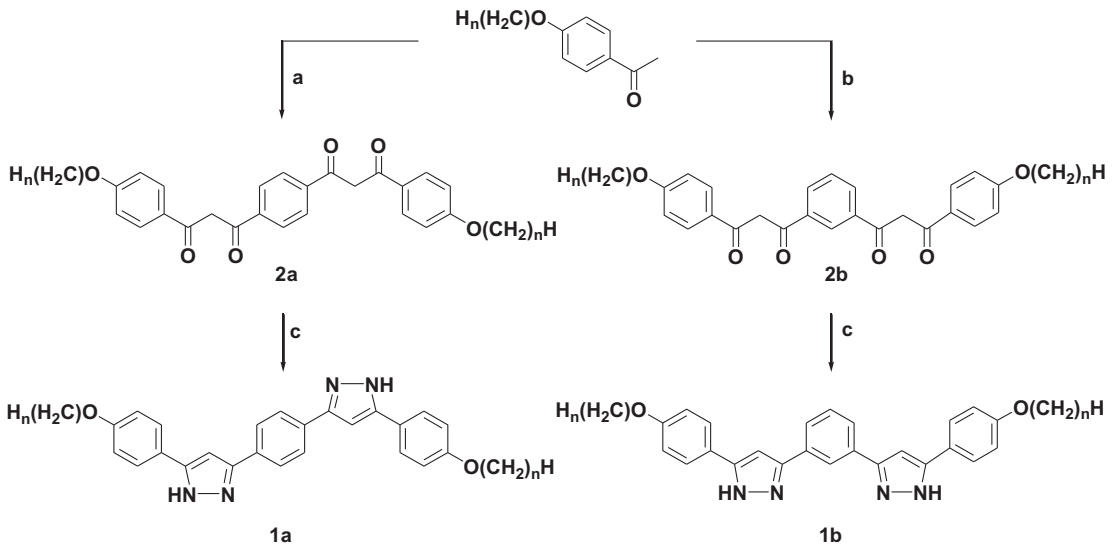

Scheme 1. Reactions and reagents. (a) Dimethyl terephthalate (0.50 equiv) in refluxing THF, 24 h, 52–68%; (b) dimethyl isophthalate (0.50 equiv) in refluxing THF, 24 h, 50–66%; (c) N_2H_4 (1.5 equiv), acetic acid (0.5 mL), refluxing in CH_2Cl_2, 24 h, 70–82%.

Table 1
Phase transition temperature (¢J) and enthalpies (Kcal/mol) of **1**–**2**

2a; n = 12					Cr	156.9 (48.1) / 150.7 (47.2)	I	
2b; n = 12					Cr	119.1 (50.4) / 105.8 (92.0)	I	
1a; n = 8	Cr	201.2 (13.2) / 186.6 (11.0)	SmC	348.8 (0.67) / 338.8 (0.42)	SmA	374.6 (7.62) / 373.8 (7.35)	I	
10	Cr	196.3 (13.6) / 189.4 (12.1)	SmC	345.4 (1.27) / 342.4 (0.88)	SmA	357.0 (6.47) / 354.8 (6.25)	I	
12	Cr	190.4 (12.8) / 184.1 (12.2)	SmC	332.1 (1.31) / 329.6 (1.25)	SmA	341.1 (5.60) / 339.1 (5.40)	I	
14	Cr	190.2 (15.8) / 185.8 (14.9)	SmC	318.5 (1.68) / 316.4 (1.66)	SmA	324.7 (4.13) / 322.7 (3.87)	I	
16	Cr	185.7 (13.5) / 180.5 (12.9)	SmC	302.9 (1.64) / 300.9 (1.56)	SmA	309.4 (2.93) / 307.6 (2.74)	I	
1b; n = 8					Cr	204.1 (36.3) / 197.2 (34.2)	I	
10					Cr	198.7 (32.9) / 190.4 (31.9)	I	
12					Cr	191.9 (31.7) / 185.1 (30.8)	I	
14					Cr	181.3 (30.6) / 174.6 (30.4)	I	

a: n = carbon length in the alkoxy chains; Cr = crystal, SmC = smectic C, SmA = smectic A phases, I = isotropic.

coplanarity of compounds **1a** over **1b**, as confirmed by single crystal X-ray crystallography. The lack of mesomorphic properties in compounds **1b** was also attributed to the slightly bent structures and poorer coplanarity of four rings in compounds **1a**. The shape effect of *para*- and *meta*-substitution on the formation of mesophases has been demonstrated also in bis(5-phenyl-1,3,4-oxadiazole-2-yl)benzene.[22c,38] They are structurally similar to **1a**–**b**, as a rod-like five-ring structure. The results indicated that the 1,3-*meta*-substituted 1,3,4-oxadiazole derivatives exhibited no mesogenic behavior, whereas, the 1,4-*para*-substituted 1,3,4-oxadiazole derivatives formed smectic-like mesophases. A clearing temperature at T_{cl}=142.8 °C and T_{cl}=224.7 °C (all *n*'s=12) was observed for 1,3- and 1,4-disubstituted benzenes, respectively. This was also due to a loss of linearity by the presence of the 1,3,4-oxadiazoles ring, for it is unable to make co-linear disubstitution bonding. No intermolecular hydrogen bonding was possible in both *meta*- and *para*-bis(1,3,4-oxadiazole-2-yl) benzenes. The importance of hydrogen bond in **1a** (*n*=8) was noted by a wider temperature range of mesophases observed by ΔT=173.4 °C over ΔT=64.3 °C in *para*-1,4-bis(5-phenyl-1,3,4-oxadiazole-2-yl) benzene (*n*=8). Compounds **1a**–**b** were all thermally stable. Thermal gravimetric analysis (TGA) revealed good thermal stability for both series of compounds **1a**–**b**. For example, the decomposition temperatures for a 5% weight loss for **1a** (*n*=14) and **1b** (*n*=8) were obtained at T_d=415.7 °C and T_d=398.5 °C, respectively (Fig. 2).

2.3. Crystal and molecular structures of 1a–14 and 1b–8

In order to understand the correlation between the molecular structures and mesomorphic behavior, two single crystals of the mesogenic **1a**–**14** and nonmesogenic **1b**–**8** suitable for crystallographic analysis were obtained by slow diffusion from THF/MeOH at room temperature and their structures resolved. Fig. 3 shows the two molecular structures with the atomic numbering schemes. Table 2 lists their crystallographic and structural refinement data for the two molecules. Compound **1a**–**14** crystallizes in a triclinic space group *P*–1 with a *Z*=1, and compound **1b**–**8** crystallizes in a monoclinic space group *C*2/*c* with a *Z*=8. The overall molecular shapes of both crystals were considered as linear-shaped or slightly bent molecules. It is well known that pyrazole has two resonant isomers,[39–42] and the pyrazoylate hydrogen (–NH) can reside on either two nitrogen atoms, which is so-called *tautomeric prototropy*.

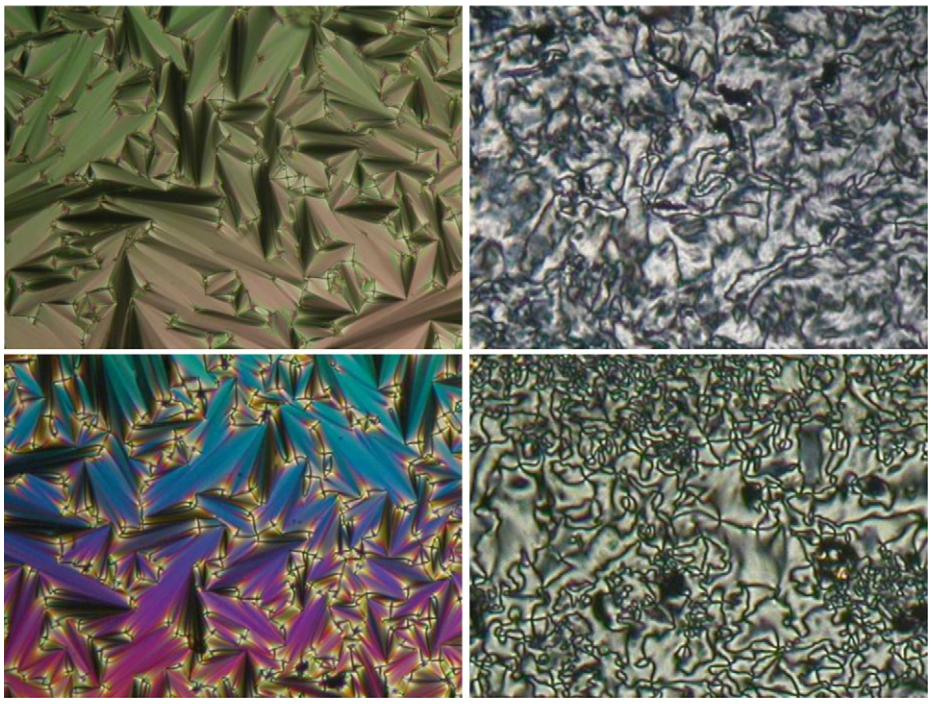

Fig. 1. Optical textures observed. Top left and right plates: SmA phase at 360.0 °C and SmC phase at 340.0 °C by **1a** (*n*=8). Bottom left and right plates: SmA phase at 320 °C and SmC phase at 312.0 °C by **1a** (*n*=14).

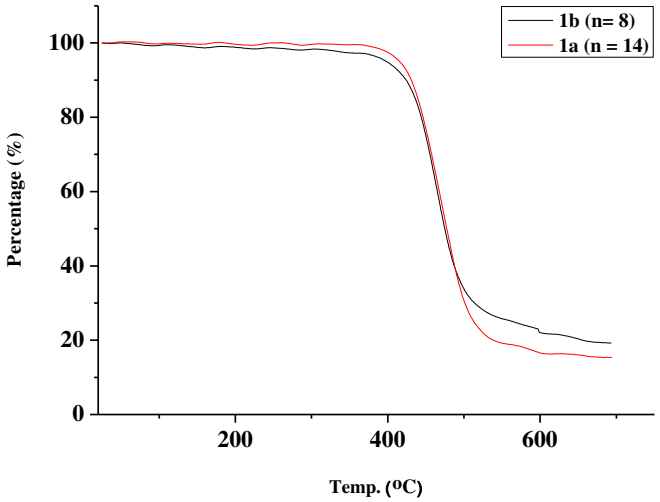

Fig. 2. TGA plots of compounds **1a**–**14** and **1b**–**8** (heating rate of 20 °C min^{-1}; N_2 atmosphere).

Table 2
Crystallographic data for crystals **1a**–**14** and **1b**–**8**

Compds.	**1a** (n=14)	**1b** (n=8)
Empirical formula	$C_{52}H_{74}N_4O_2$	$C_{40}H_{50}N_4O_2$
Formula weight	787.15	618.84
T/K	200(2)	200(2)
Crystal system	Triclinic	Monoclinic
Space group	P–1	$C2/c$
a/Å	10.1536(7)	35.9910(5)
b/Å	10.5977(5)	15.8385(2)
c/Å	12.0042(9)	13.0469(1)
α/°	76.231(5)	90
β/°	85.607(4)	109.9196(7)
γ/°	64.400(4)	90
U/Å^3	1130.92(13)	6992.34(14)
Z	1	8
F(000)	430	2672
D_{calcd}/Mg m^{-3}	1.156	1.176
Crystal size/mm^3	0.40×0.13×0.11	0.55×0.50×0.12
Range for data collection/°	1.75 to 25.00	1.42 to 27.50
Reflection collected	11,809	24,966
Data, restraints, parameters	3955/0/263	7969/45/409
Independent reflection	3955 [$R_{(int)}$=0.0700]	7969 [$R_{(int)}$=0.0340]
Final $R1$, $wR2$	0.0665, 0.1862	0.0732, 0.2015

This process has been found to be fast in solution at room temperature. A pair of isomeric structures was observed in some pyrazoles. Crystallographic data showed that for both compounds **1a**–**14** and **1b**–**8**, the molecules contain only one independent bis-pyrazole molecule. The two protons of the pyrazole group only reside at the nitrogen atom N2 and N4 in **1b**–**8**, and N2 in **1a**–**14**, adjacent to the side phenyl groups. The two N–N bond lengths in crystal **1a**–**14** were equal, whereas, they are nearly equal (i.e., Δ=0.0135 Å) in crystal **1b**–**8**. All the C–N bond lengths [1.3366(46)–1.3506(31) Å] in both crystals are almost equal, and are shorter than the normal single bond (C–N; 1.47–1.50 Å), but close to that of double bond (C=N; 1.28–1.33 Å), indicating that electron density was considerably delocalized on both pyrazoyl rings.

Interestingly, the conformations of two pyrazoles were apparently distinct; they adopt a trans-conformation in **1a**–**14** and a *cis*-conformation in **1b**–**8**. The five rings; two pyrazoyl rings and three phenyl rings in **1a**–**14** were in fact coplanar, whereas, all five rings were not coplanar in **1b**–**8**. The measured two dihedral angle between the two pyrazole rings and central phenylene rings in **1b**–**8** are 18.677(83)° and −25.257(71)°, making a total dihedral angle of 41.395(91)° for two pyrazole rings, resulting in a non-planar conformation in **1b**–**8**. Notably, an *intermolecular* H-bond between pyrazoyl rings was formed in both crystals. However, a traditional dimeric structure induced by H-bonds often observed in a style of mono-pyrazole was not formed. Instead, the first pyrazoyl ring (–N*H*) in each molecule separately formed hydrogen bonds with another pyrazole ring (for example, –N2*H*2···*N*1 in **1a**–**14**) of the neighboring molecule by a *trans*-conformation. H-bond was then alternately formed, leading to an infinite Zigzag chain in one direction. A bond distance of 2.17 Å [∠140.263(153)°] in **1a**–**14**, and 2.09 Å [∠140.230(126)° & 132.334(136)] and 2.09 Å in **1b**–**8** was obtained (Fig. 4). All H-bonds linked together as a pseudo polymeric supramolecular structure (Fig. 5) formed in both crystals. The details about the H-bonding are presented in Table 3. A weak π–π interaction (C7–C12···H3, as offset face to face alignment) with a perpendicular distance of ~3.45 Å was also observed in **1a**–**14**. However, no π–π interaction was observed in **1b**–**8**. The π–π interaction may also play an important role in controlling the formation/induction of mesophases (Fig. 6).

2.4. Variable temperature powder X-ray diffractions

Variable-temperature powder XRD diffraction experiments were conducted to confirm the structures of the mesophases of compound **1a**. Fig. 7 shows diffraction plots for **1a** (n=14) at 25 °C, 250 °C and 320 °C. A d-spacing of ~29.70 Å was obtained at room temperature, which was quite close to ~29.52 Å calculated from crystallographic data. It was also close to the half of a molecular length (~56.82 Å) as the repeated distance. Upon cooling from clearing temperature to T=320 °C, a typical diffraction pattern with one very strong diffraction peak at ~42.69 Å was observed. This peak corresponded to a layer structure, assigned as Miller indices 100. Furthermore, a very broad weak peak of ~4.86 Å at wide angle

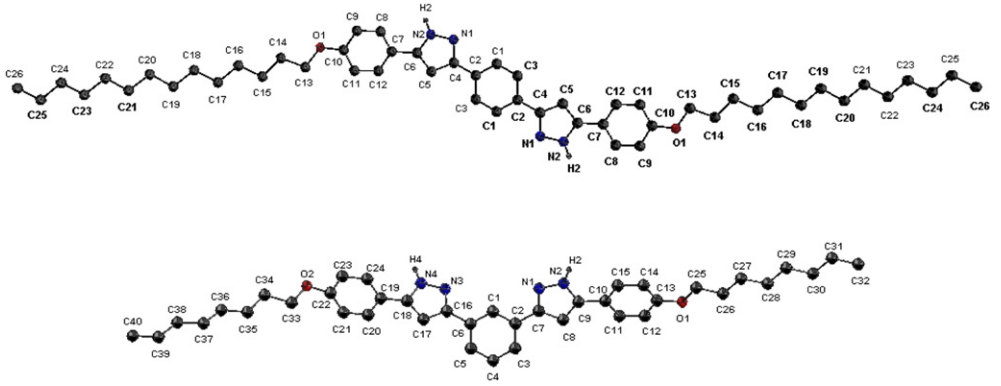

Fig. 3. Two ORTEP plots for compounds **1a**–**14** (top plot) and **1b**–**8** with the numbering schemes.

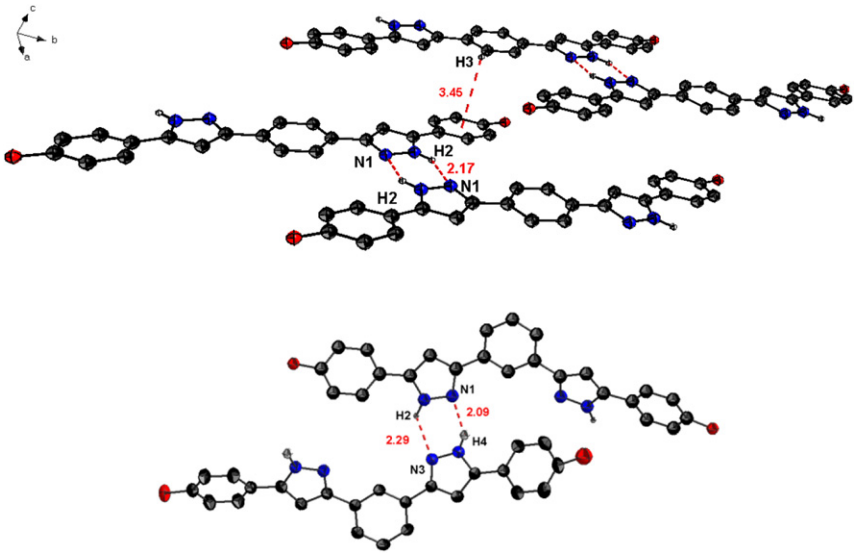

Fig. 4. The hydrogen bonds formed in **1a**–**14** (top) and **1b**–**8** (bottom); N1–H4=2.09 Å and N3–H2=2.29 Å.

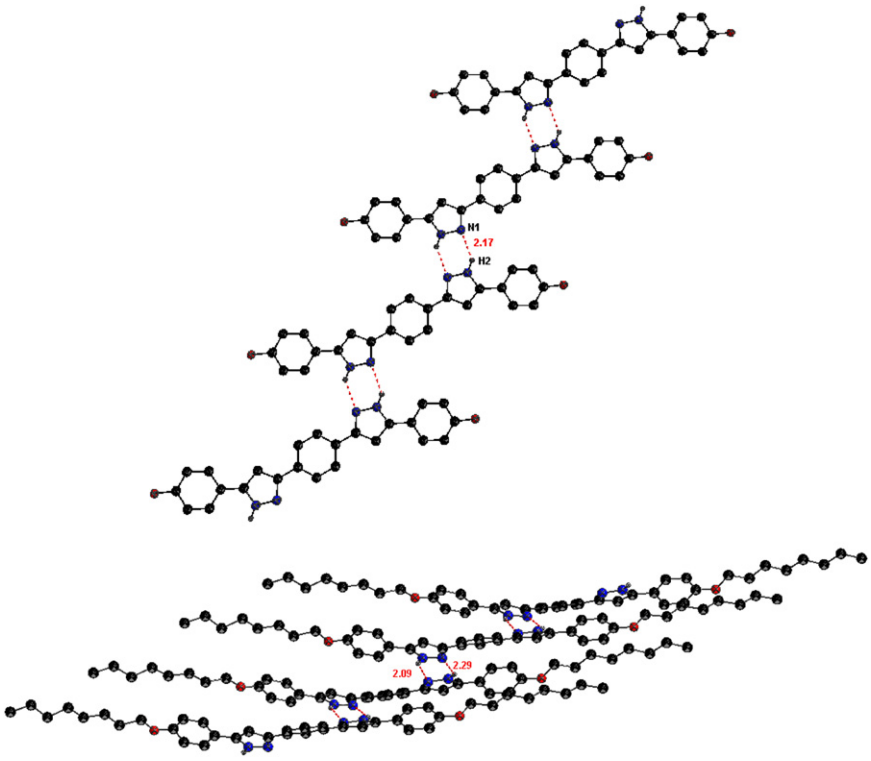

Fig. 5. Pseudo-polymeric structures in **1a**–**14** (top) and **1b**–**8** (bottom).

Table 3
Hydrogen-bonding geometry and π–π interaction in **1a**–**14** and **1b**–**8**

Compd	Mesophase	D–H···A	*d*(D–H)	*d*(H···A)	*d*(D···A)	∠(DHA)/°	π–π interaction
1a–**14**	SmA/SmC	N(2)–H_{N2}···N(1)	0.88	2.17	2.90	140.263(153)	3.45
1b–**8**	Cr	N(2)–H_{N2}···N(3)	0.88	2.29	2.95	132.334(136)	None
		N(4)–H_{N4}···N(1)	0.88	2.09	2.83	140.230(126)	

Distances unit in Å.

region was due to halo diffraction. This diffraction pattern was typically characteristic of a layer structure observed for a SmA phase. Within the layers of SmA phase, the long axes of the molecules lie parallel to one another, their direction being normal to the plane of the layer. The layer *d*-spacing of ~42.69 Å is much smaller than the molecular length of 56.68 Å obtained from crystallographic data, indicating that the terminal alkoxy chains in SmA phase were probably interdigitated to some extent and leading to

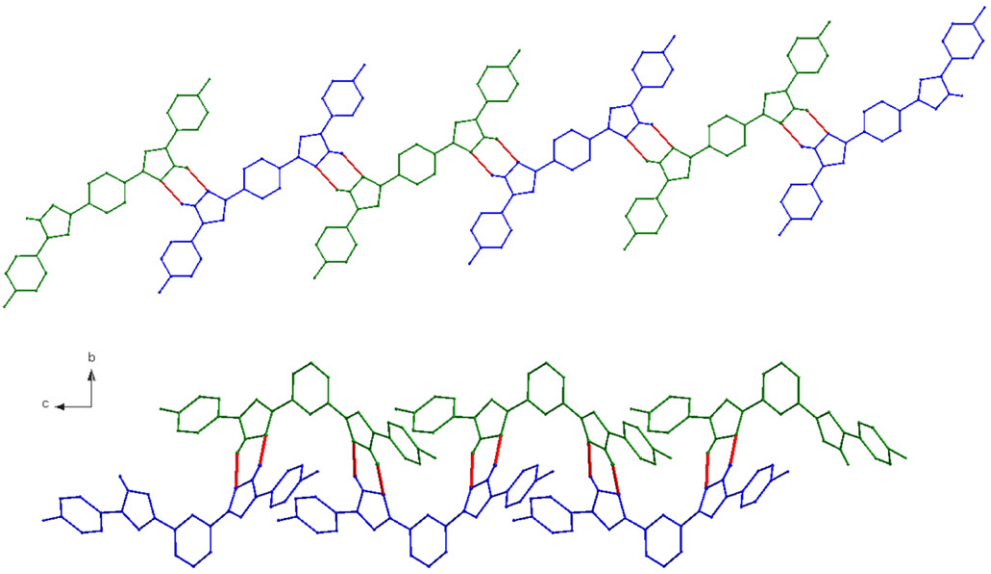

Fig. 6. Intermolecular organization through an infinite zigzag chain formed by H-bonds along the axis in **1a**–**14** (top) and **1b**–**8** (bottom).

a smaller *d*-spacing than that at 25 °C. Upon further cooling to 250 °C, a diffraction pattern with one strong of ~39.80 Å and another much weaker peak of ~20.01 Å was observed, which were assigned to 001 and 002 indices for a SmC phase. In the SmC phase, the molecules are tilted with respect to the planes of the layers. Therefore, the *d*-spacing in SmC phase is expected to be slightly than that in SmA phase. A very broad and weak peak at ~4.78–4.86 Å was observed, and this peak was assigned to the molten alkoxy chains. The molecular arrangement in crystal, smectic C and smectic A phases was proposed in Fig. 8.

3. Conclusions

The molecular geometry is an important variable in the above two series of nonlinear, all aromatic five-rings liquid crystals affecting the thermal temperatures, while the mesophase formation may be controlled by attractive electrostatic interaction. The study also demonstrated the use of hydrogen bonding to construct the extended linear polymeric structures in isomeric bis-pyrazoles **1a**–**b**. X-ray crystallographic data indicated a better molecular co-linearity of five-ring structure and π–π interaction was formed in **1a** over **1b**, which apparently faciliated the formation of layer structures of SmA/SmC phase observed in **1a**.

4. Experimental

4.1. General materials and methods

All chemicals and solvents were reagent grade from Aldrich Chemical Co., and all solvents were dried by standard techniques. ^{1}H and ^{13}C NMR spectra were measured on a Bruker DRS-200. DSC thermographs were carried out on a Mettler DSC822 and calibrated with a pure indium sample. All phase transitions are determined by a scan rate of 10.0 °C/min. Optical polarized microscopy was carried out on Zeiss Axioplan 2 equipped with a hot stage system of Mettler FP90/FP82HT. Elemental analyses were performed on a Heraeus CHN–O–Rapid elemental analyzer. The powder diffraction data were collected from the Wiggler-A beam line of the National Synchrotron Radiation Research Center (NSRRC) with the wavelength of 1.3263 Å. The powder samples were charged in Lindemann capillary tubes (80 mm long and 0.01 mm thick) from Charles Supper Co. with an inner diameter of 1.0 mm.

4.2. Single crystal X-ray crystallography and powder XRD diffractometry

X-ray diffraction data were collected at 200 (2) K on a Nonius Kappa CCD X-ray diffractometer unit using graphite-mono chromated Mo Kα radiation (λ=0.71073 Å) from crystals mounted on glass fibers and quickly coated in epoxy resin. Cell parameters were retrieved and refined using DENZO-SMN software on all observed reflections. Data reduction was performed with the DENZOSMN software. The program package SHELXTL was used for space group determination, structure solution, and refinement. Refinement was performed against F2 by weighted full-matrix least-square, and empirical absorption correction (SADABS) was applied. H atoms were placed at calculated positions using suitable riding models with isotropic displacement parameters derived from their carrier atoms. The powder diffraction data were collected from the Wiggler-A beam line of the National Synchrotron Radiation Research Center with a wavelength of 1.3263 Å.

4.3. Synthetic preparation of the compounds 1a–b

*4.3.1. (2Z,2′Z)-1,1′-(1,3-Phenylene)bis(3-(4-(dodecyloxy)phenyl)-3-hydroxyprop-2-en-1-one) **2b** (n=12).* The solution of 4-dodecyloxyacetophenone (3.00 g, 9.02 mmol) and NaH (0.648 g, 0.027 mol) dissolved in 30 mL of dry THF or DME was stirred for 20 min under nitrogen atmosphere. The solution was gently heated to refluxing temperature, and stirred for 30 min. The solution was turned deep red. The solution of dimethyl isophthalate (0.875 g, 4.51 mmol) dissolved in 15 mL of THF was dropwise added, and the solution was then refluxed for 24 h. The solution was cooled and quenched carefully with distilled water. The dilute aqueous HCl (1.0 M) was added to raise the pH of the solution to acidic side. The solution was extracted twice with 50 mL of CH_2Cl_2/H_2O (1/1). The organic layers were collected and dried over $MgSO_4$. The products isolated as pale yellow solid were obtained by recrystallization from acetone/THF or CH_3OH/THF. Yield 58–71%. ^{1}H NMR ($CDCl_3$): δ 0.86 (t, J=6.6 Hz, $-CH_3$, 6H), 1.25–1.45 (m, $-CH_2$, 40H), 1.77–1.82 (m, $-CH_2$, 4H), 4.01 (t, J=6.5 Hz, $-OCH_2$, 4H), 6.84 (s, –CH, 2H), 6.94

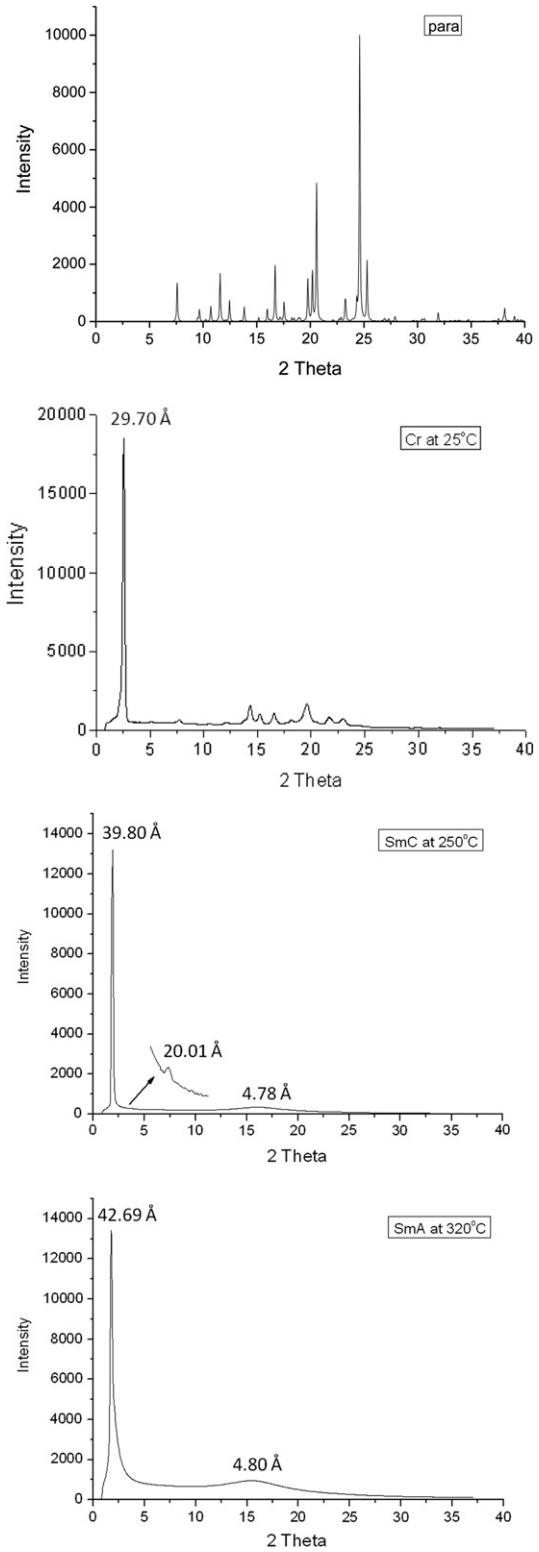

Fig. 7. Variable-temperature powder XRD diffraction plots of **1a**–**14**. From top to bottom: the theoretical pattern calculated from the X-ray crystallographic data, at room temperature, at 250 °C and 320 °C.

(d, *J*=9.0 Hz, Ar–H, 4H), 7.55 (t, *J*=7.8 Hz, Ar–H, 1H), 7.96 (d, *J*=8.7 Hz, Ar–H, 4H), 8.08 (d, *J*=6.6 Hz, Ar–H, 2H), 8.51 (s, Ar–H, 1H), 17.02 (s, –OH, 2H). ^{13}C NMR ($CDCl_3$): δ 13.12, 21.68, 24.99, 28.12, 28.35, 28.58, 28.64, 30.91, 67.33, 91.58, 113.51, 124.44, 126.60, 128.00, 128.45, 129.33, 135.22, 162.11, 182.07, 185.43.

4.3.2. (2Z,2′Z)-1,1′-(1,3-Phenylene)bis(3-(4-(decyloxy)phenyl)-3-hydroxyprop-2-en-1-one) ***2b*** *(n=10).* Light yellow solid, yield 55%. ^{1}H NMR ($CDCl_3$): δ 0.88 (t, *J*=6.3 Hz, –CH_3, 6H), 1.25–1.47 (m, –CH_2, 32H), 1.75–1.84 (m, –CH_2, 4H), 4.00 (t, *J*=6.6 Hz, –OCH_2, 4H), 6.81 (s, –CH, 2H), 6.84 (d, *J*=7.8 Hz, Ar–H, 4H), 7.58 (t, *J*=7.8 Hz, Ar–H, 1H), 7.96 (d, *J*=8.7 Hz, Ar–H, 4H), 8.09 (d, *J*=6.6 Hz, Ar–H, 2H), 8.51 (s, Ar–H, 1H), 17.02 (s, –OH, 2H). ^{13}C NMR ($CDCl_3$): δ 14.10, 22.68, 25.98, 29.11, 29.34, 29.56, 29.58, 29.63, 31.90, 68.33, 92.59, 114.51, 125.44, 127.61, 129.00 129.45, 130.32, 136.23, 163.11, 183.09, 186.43.

4.3.3. (2Z,2′Z)-1,1′-(1,4-Phenylene)bis(3-hydroxy-3-(4-(octyloxy) phenyl)prop-2-en-1-one) ***2a*** *(n=8).* Yellow solid, yield 70%. ^{1}H NMR ($CDCl_3$): δ 0.87 (t, *J*=6.6 Hz, –CH_3, 6H), 1.28–1.48 (m, –CH_2, 40H), 1.75–1.85 (m, –CH_2, 4H), 4.02 (t, *J*=6.6 Hz, –OCH_2, 4H), 6.83 (s, –CH, 2H), 6.95 (d, *J*=8.7 Hz, Ar–H, 4H), 7.96 (d, *J*=9.0 Hz, Ar–H, 4H), 8.04 (s, Ar–H, 4H), 16.87 (s, –OH, 2H). ^{13}C NMR ($CDCl_3$): δ 14.31, 22.88, 26.22, 29.34, 29.55, 32.03, 68.59, 93.24, 114.77, 127.38, 128.10, 129.74, 130.62, 138.77, 163.41, 187.47.

4.3.4. (2Z,2′Z)-1,1′-(1,4-Phenylene)bis(3-(4-(dodecyloxy)phenyl)-3-hydroxyprop-2-en-1-one) ***2a*** *(n=12).* Yellow solid, yield 75%. ^{1}H NMR ($CDCl_3$): δ 0.86 (t, *J*=6.5 Hz, –CH_3, 6H), 1.31–1.56 (m, –CH_2, 36H), 1.75–1.84 (m, –CH_2, 4H), 4.02 (t, *J*=6.5 Hz, –OCH_2, 4H), 6.82 (s, –CH, 2H), 6.94 (d, *J*=8.7 Hz, Ar–H, 4H), 7.95 (d, *J*=8.7 Hz, Ar–H, 4H), 8.04 (s, Ar–H, 4H), 16.92 (s, –OH, 2H). ^{13}C NMR ($CDCl_3$): δ 14.34, 22.92, 26.21, 29.34, 29.58, 29.80, 29.87, 32.14, 68.58, 93.22, 114.75, 127.36, 128.08, 129.73, 138.75, 163.40, 182.03, 187.46.

4.3.5. (2Z,2′Z)-1,1′-(1,4-Phenylene)bis(3-hydroxy-3-(4-(tetra decyloxy)phenyl)prop-2-en-1-one) ***2a*** *(n=14).* Yellow solid, yield 78%. ^{1}H NMR ($CDCl_3$): δ 0.86 (t, *J*=6.8 Hz, –CH_3, 6H), 1.18–1.54 (m, –CH_2, 44H), 1.78–1.85 (m, –CH_2, 4H), 4.02 (t, *J*=6.6 Hz, –OCH_2, 4H), 6.83 (s, –CH, 2H), 6.95 (d, *J*=9.0 Hz, Ar–H, 4H), 7.96 (d, *J*=9.0 Hz, Ar–H, 4H), 8.04 (s, Ar–H, 4H), 16.93 (s, –OH, 2H).

4.3.6. (2Z,2′Z)-1,1′-(1,4-Phenylene)bis(3-(4-(hexadecyloxy)phenyl)-3-hydroxyprop-2-en-1-one) ***2a*** *(n=16).* Yellow solid, yield 72%. ^{1}H NMR ($CDCl_3$): δ 0.86 (t, *J*=6.6 Hz, –CH_3, 6H), 1.71–1.62 (m, –CH_2, 52H), 1.75–1.82 (m, –CH_2, 4H), 4.02 (t, *J*=6.5 Hz, –OCH_2, 4H), 6.83 (s, –CH, 2H), 6.95 (d, *J*=8.7 Hz, Ar–H, 4H), 7.96 (d, *J*=9.0 Hz, Ar–H, 4H), 8.04 (s, Ar–H, 4H), 16.93 (s, –OH, 2H). ^{13}C NMR ($CDCl_3$): δ 14.35, 22.91, 26.21, 29.33, 29.59, 29.81, 29.91, 32.15, 68.57, 93.22, 114.75, 127.36, 129.73, 138.75, 163.40, 163.40, 182.03, 187.47.

4.3.7. 1,3-Bis(5-(4-(dodecyloxy)phenyl)-1H-pyrazol-3-yl)benzene ***1b*** *(n=12).* The solution of (2Z,2′Z)-1,1′-(1,3-phenylene)bis(3-(4-(dodecyloxy)phenyl)-3-hydroxyprop-2-en-1-one) (1.00 g) dissolved in 30 mL THF was slowly added 0.5 mL of glacial acetic acid and the solution was stirred for 5 min. Then the hydrazine (1.0 mL) was added and refluxed for 24 h. The solution was concentrated to dryness, and the products isolated as white solid were obtained by recrystallization from THF/CH_3OH (hot). Yield 70%. ^{1}H NMR (DMSO-d_6): δ 0.82 (m, –CH_3, 6H), 1.24–1.39 (m, –CH_2, 36H), 1.70–1.72 (m, –CH_2, 4H), 4.01 (t, *J*=6.3 Hz, –OCH_2, 4H), 7.00 (m, Ar–H, 4H), 7.15 (s, –CH, 2H), 7.50 (m, Ar–H, 1H), 7.75 (m, Ar–H, 6H), 8.29 (s, Ar–H, 1H), 10.25 (s, –NH), 10.71 (s, –NH), 13.23 (m, –NH, 2H). Anal. Calcd for $C_{48}H_{66}N_4O_2$: C, 78.86; H, 9.10. Found C, 78.58; H, 9.18.

4.3.8. 1, 3-Bis(5-(4-(octyloxy)phenyl)-1H-pyrazol-3-yl)benzene ***1b*** *(n=8).* White solid, yield 58%. ^{1}H NMR (THF-d_6): δ 0.91 (t, *J*=5.4 Hz, –CH_3, 6H), 1.32–1.50 (m, –CH_2, 20H), 1.73–1.81 (m, –CH_2, 4H), 3.99 (t, *J*=6.5 Hz, –OCH_2, 4H), 6.69 (s, –CH, 2H), 7.41

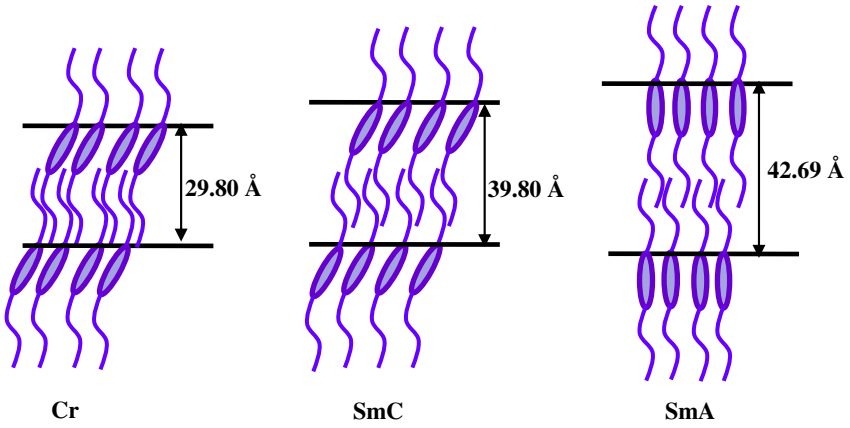

Fig. 8. The molecular arrangements proposed in Cr, SmC and SmA phases formed in **1a**.

(t, *J*=7.7 Hz, Ar–H, 1H), 7.70 (d, *J*=6.9 Hz, Ar–H, 6H), 8.29 (s, Ar–H, 1H), 10.91 (s, –NH), 12.37 (s, –OH, 2H). Anal. Calcd for $C_{40}H_{50}N_4O_2$: C, 77.63; H, 8.14. Found C, 77.61; H, 8.19.

4.3.9. 1, 3-Bis(5-(4-(tetradecyloxy)phenyl)-1H-pyrazol-3-yl)benzene ***1b*** *(n=14).* White crystal, yield 50%. Anal. Calcd for $C_{52}H_{74}N_4O_2$: C, 79.34; H, 9.46. Found C, 79.23; H, 9.44. The ^{1}H and ^{13}C NMR data were not obtained due to poor solubility.

4.3.10. 1, 3-Bis(5-(4-(decyloxy)phenyl)-1H-pyrazol-3-yl)benzene ***1b*** *(n=10).* White solid, yield 52%. ^{1}H NMR (DMSO-d_6): δ 0.85 (t, *J*=6.6 Hz, $-CH_3$, 6H), 1.24–1.42 (m, $-CH_2$, 28H), 1.70–1.74 (m, $-CH_2$, 4H), 4.00 (t, *J*=6.2 Hz, $-OCH_2$, 4H), 6.94 (m, Ar–H, 4H), 7.15 (s, –CH, 2H), 7.41 (t, *J*=7. 7 Hz, Ar–H, 1H), 7.67 (m, Ar–H, 6H), 8.29 (s, Ar–H, 1H), 13.23 (m, –NH, 2H). ^{13}C NMR (THF-d_6): δ 14.59, 23.72, 27.22, 30.47, 30.57, 30.72, 33.03, 99.52, 99.52, 115.50, 125.31, 127.44, 160.21. Anal. Calcd for $C_{44}H_{58}N_4O_2$: C, 78.30; H, 8.66. Found C, 78.21; H, 8.80.

4.3.11. 1,4-Bis(5-(4-(hexadecyloxy)phenyl)-1H-pyrazol-3-yl)benzene ***1a*** *(n=16).* White solid, yield 73%. The ^{1}H NMR spectra are not obtained due to poor solubility. Anal. Calcd for $C_{56}H_{82}N_4O_2$: C, 79.76; H, 9.80. Found C, 79.64; H, 9.78.

4.3.12. 1,4-Bis(5-(4-(tetradecyloxy)phenyl)-1H-pyrazol-3-yl)benzene ***1a*** *(n=14).* White solid, yield 73%. The ^{1}H NMR spectra are not obtained due to poor solubility. Anal. Calcd for $C_{52}H_{74}N_4O_2$: C, 79.34; H, 9.48. Found C, 79.35; H, 9.54.

4.3.13. 1,4-Bis(5-(4-(dodecyloxy)phenyl)-1H-pyrazol-3-yl)benzene ***1a*** *(n=12).* White crystal, yield 75%. ^{1}H NMR (DMSO-d_6): δ 0.85 (t, *J*=6.6 Hz, $-CH_3$, 6H), 1.25–1.47 (m, $-CH_2$, 36), 1.70–1.74 (m, $-OCH_2CH_2$, 4H), 4.00 (t, *J*=6.3 Hz, $-OCH_2$, 4H), 6.99 (d, *J*=8.4 Hz, Ar–H, 4H), 7.11 (s, –CH, 2H), 7.73 (d, *J*=8.4 Hz, Ar–H, 4H), 7.89 (s, Ar–H, 4H), 10.25 (s, –NH), 10.71 (s, –NH), 13.27 (s, –NH). Anal. Calcd for $C_{48}H_{66}N_4O_2$: C, 78.86; H, 9.10. Found C, 78.63; H, 9.15.

4.3.14. 1,4-Bis(5-(4-(decyloxy)phenyl)-1H-pyrazol-3-yl)benzene ***1a*** *(n=10).* White solid, yield 70%. ^{1}H NMR (DMSO-d_6): δ 0.86 (t, *J*=6.5 Hz, $-CH_3$, 6H), 1.26–1.42 (m, $-CH_2$, 28H), 1.68–1.77 (m, $-CH_2$, 4H), 3.99 (t, *J*=6.3 Hz, $-OCH_2$, 4H), 6.99 (d, *J*=8.1 Hz, Ar–H, 4H), 7.11 (s, –CH, 2H), 7.73 (d, *J*=8.1 Hz, Ar–H, 4H), 7.89 (s, Ar–H, 4H), 10.25 (s, –NH), 10.71 (s, –NH), 13.25 (s, –NH). Anal. Calcd for $C_{44}H_{58}N_4O_2$: C, 78.30; H, 8.66. Found C, 78.35; H, 8.30.

4.3.15. 1,4-Bis(5-(4-(octyloxy)phenyl)-1H-pyrazol-3-yl)benzene ***1a*** *(n=8).* White solid, yield 70%. ^{1}H NMR spectra are not available due to poor solubility. Anal. Calcd for $C_{40}H_{50}N_4O_2$: C, 77.63; H, 8.14. Found C, 77.60; H, 8.21.

Acknowledgements

We thank the National Science Council of Taiwan, ROC (NSC 100-2113-M-008-003-MY2) in generous support of this work.

References and notes

1. Coco, S.; Cordovilla, C.; Domínguez, D.; Donnio, B.; Espinet, P.; Guillon, D. *Chem. Mater.* **2009**, *21*, 3282–3289.
2. Lavigueur, C.; Foster, E. J.; Williams, V. E. *J. Am. Chem. Soc.* **2008**, *130*, 11791–11800.
3. Kutsumizu, S.; Mori, H.; Fukatami, M.; Naito, S.; Sakajiri, K.; Saito, K. *Chem. Mater.* **2008**, *20*, 3675–3687.
4. Barberá, B.; Puig, L.; Romero, P.; Serrano, J. L.; Sierra, T. *J. Am. Chem. Soc.* **2006**, *128*, 4487–4492.
5. Miao, J.; Zhu, L. *Chem. Mater.* **2010**, *22*, 197–206.
6. Saez, I. M.; Goodby, J. W. *J. Mater. Chem.* **2005**, *15*, 26–40.
7. Desiraju, G. R. *Angew. Chem., Int. Ed.* **2007**, *46*, 8342–8356.
8. Grabowski, S. J. *Chem. Rev.* **2011**, *111*, 2597–2625.
9. Vera, F.; Serrano, J. L.; Sierra, T. *Chem. Soc. Rev.* **2009**, *38*, 781–796.
10. Giménez, R.; Elduque, A.; López, J. A.; Barberá, J.; Cavero, E.; Lantero, L.; Oro, L. A.; Serrano, J. L. *Inorg. Chem.* **2006**, *45*, 10363–10370.
11. Massiot, P.; Impèror-Clerc, M.; Veber, M.; Deschenaux, M. *Chem. Mater.* **2005**, *17*, 1946–1951.
12. Ziessel, R.; Pickaert, G.; Camerel, F.; Donnio, B.; Guillon, D.; Cesario, C.; Prange, T. *J. Am. Chem. Soc.* **2004**, *126*, 12403–12413.
13. Elguero, J.; Goya, P.; Jagerovic, N.; Silva, A. M. S. Pyrazoles as Drugs: Facts and Fantasies In; Attanasi, O. A., Spinelli, D., Eds. . *Targets in Heteroyclic Systems*; Italian Society of Chemistry: Roma, 2002; Vol. 6, pp 52–98.
14. Trofimenko, S. *Chem. Rev.* **1972**, *72*, 497–509.
15. Niedenzu, K.; Trofimenko, S. *Top. Curr. Chem.* **1986**, *131*, 1–37.
16. Reedijk, J. In; Wilkinson, G., Gillard, R. D., McCleverty, J. A., Eds. *Comprehensive Coordination Chemistry*; Pergamon: Oxford, 1987; Vol. 2.
17. Viciano-Chumillas, M.; Tanase, S.; de Jongh, L. J.; Reedijk, J. *Eur. J. Inorg. Chem.* **2010**, 3403–3418.
18. Halcrow, M. A. *Dalton Trans.* **2009**, 2059–2073.
19. Zhou, Y.; Chen, W.; Wang, D. *Dalton Trans.* **2008**, 1444–1453.
20. Perez, J.; Riera, L. *Eur. J. Inorg. Chem.* **2009**, 4913–4925.
21. (a) Wang, D. J.; Zheng, C. Y.; Fan, L. *J. Mol. Struct.* **2009**, *938*, 311–315; (b) Zheng, C. Y.; Wang, D. J. *Struct. Chem.* **2010**, *21*, 1043–1049.
22. (a) Jozak, T.; Zabel, D.; Schubert, A.; Sun, Y.; Thiel, W. R. *Eur. J. Inorg. Chem.* **2010**, 5135–5145; (b) Bergner, S.; Wolmershauser, G.; Kelm, H.; Thiel, W. R. *Inorg. Chim. Acta* **2008**, *361*, 2059–2069; (c) Sanz, D.; Claramunt, R. M.; Alkorta, I.; Elguero, J.; Thiel, W. R.; Ruffer, T. *New J. Chem.* **2008**, *32*, 2225–2232.
23. Barbert, J.; Gimenz, R.; Serrano, J. L.; Alcala, R.; Villacampa, B.; Villalba, J.; Ledoux, I.; Zyss, J. *Liq. Cryst.* **1997**, *22*, 265–273.
24. Shen, W. C.; Wang, Y. J.; Cheng, K. L.; Lee, G. H.; Lai, C. K. *Tetrahedron* **2006**, *62*, 8035–8044.
25. Chen, Y.; Harrison, W. T. A.; Imrie, C. T.; Ryder, K. S. *J. Mater. Chem.* **2002**, *12*, 579–585.
26. Barbera, J.; Gimnenez, R.; Serrano, J. L. *Chem. Mater.* **2000**, *12*, 481–489.
27. Gimenez, R.; Manrique, A. B.; Uriel, S.; Barbera, J.; Serrano, J. L. *Chem. Commun.* **2004**, 2064–2065.
28. Liao, C. T.; Chen, H. H.; Hsu, H. F.; Poloek, A.; Chi, H. H. Y.; Wang, K. W.; Lai, C. H.; Lee, G. H.; Shih, C. W.; Chou, P. T. *Chem.—Eur. J.* **2011**, *17*, 546–556.

29. Barbera, J.; Lantero, I.; Moyano, S.; Serrano, J. L.; Elduque, A.; Gimenez, R. *Chem.—Eur. J.* **2010**, *16*, 14545–14553.
30. (a) Chen, M. C.; Lee, S. C.; Ho, C. C.; Hu, T. S.; Lee, G. G.; Lai, C. K. *Tetrahedron* **2009**, *65*, 9460–9467; (b) Chou, S. Y.; Chen, C. J.; Tsai, S. L.; Sheu, H. S.; Lee, G. H.; Lai, C. K. *Tetrahedron* **2009**, *65*, 1130–1139.
31. (a) Mayoral, M. J.; Ovejro, P.; Campo, J. A.; Heras, J. V.; Pinilla, E.; Torres, M. R.; Lodeiro, C.; Cano, M. *Dalton Trans.* **2008**, 6912–6924; (b) Kishimura, A.; Yamashits, T.; Aida, T. *J. Am. Chem. Soc.* **2005**, *127*, 179–183.
32. Fustero, S.; Sanchez-Rosello, M.; Barrio, P.; Simon-Fuentes, A. *Chem. Rev.* **2011**, *111*, 6984–7034.
33. Clegg, J. K.; Gloe, K.; Hayter, M. J.; Kataeva, O.; Lindoy, L. F.; Moubaraki, B.; McMurtrie, J. C.; Murray, K. S.; Schilter, D. *Dalton Trans.* **2006**, 3977–3984.
34. Heller, S. T.; Natarajan, S. R. *Org. Lett.* **2006**, *8*, 2675–2687.
35. Vanier, C.; Wagner, A.; Mioskowski, C. *J. Comb. Chem.* **2004**, *6*, 846–850.
36. Stauffer, S. R.; Katzenellenbogen, J. A. *J. Comb. Chem.* **2000**, *2*, 318–329.
37. Xiao, L. X.; Luo, Y. M.; Chen, Z.; Li, J.; Tang, R. R. *Spectrochim. Acta, Part A* **2008**, *71*, 321–325.
38. Cristiano, R.; Pereira, D. M.; Santos, D. O.; Gallardo, H. *Liq. Cryst.* **2005**, *32*, 7–14.
39. Acierno, D.; Concilio, S.; Diodati, A.; Iannelli, P.; Piotto, S. P.; Scarfato, P. *Liq. Cryst.* **2002**, *29*, 1383–1392.
40. Cornago, P.; Cabildo, P.; Claramunt, R. M.; Bouissane, L.; Pinilla, E.; Torres, M. R.; Elguero, J. *New J. Chem.* **2009**, *33*, 125–135.
41. Yu, W. S.; Cheng, C. C.; Cheng, Y. M.; Wu, P. C.; Song, Y. H.; Chi, Y.; Chou, P. T. *J. Am. Chem. Soc.* **2003**, *125*, 10800–10801.
42. Alkorta, I.; Blanco, F.; Elguero, J. *Struct. Chem.* **2008**, *19*, 191–198.